analytical chemistry

pubs.acs.org/ac Article

High-Fidelity CRISPR/Cas13a *trans*-Cleavage-Triggered Rolling Circle Amplified DNAzyme for Visual Profiling of MicroRNA

Ting Zhou, Mengqi Huang, Jinqiong Lin, Ru Huang,* and Da Xing*

Cite This: *Anal. Chem.* 2021, 93, 2038−2044 Read Online

ACCESS | Metrics & More | Article Recommendations | Supporting Information

ABSTRACT: The clustered regularly interspaced short palindromic repeats (CRISPR) and CRISPR-associated (Cas) (CRISPR/Cas) system innovates a next-generation biosensor due to its high-fidelity, programmability, and efficient signal amplification ability. Developing a CRISPR/Cas-based visual detection system could contribute to point-of-care biomarker diagnosis. Existing CRISPR/Cas9-mediated visual detection methods are limited by the inherent properties of Cas9. Herein, we explored the *trans*-cleavage ability of Cas13a on ribonucleotide-bearing DNA oligo, eliminated the unavailability of the *trans*-cleavage substrate for subsequent polymerization reaction, and developed a homogeneous CRISPR/Cas13a-based visual detection system (termed vCas) for specific and sensitive detection of miRNA. The results indicated that vCas can provide a detection limit of 1 fM for miR-10b with single-base specificity and can be used to analyze miRNA in serum and cell extracts. Conclusively, vCas holds a great application prospective for clinical molecular diagnosis.

Microbial clustered regularly interspaced short palindromic repeats (CRISPR) and CRISPR-associated (Cas) protein is an adaptive immune system of bacteria and archaea against invading genetic elements by CRISPR RNA (crRNA)-guided Cas endonucleases,[1] which is harnessed to be a prominent tool not only for transcription regulation and gene editing[2−4] but also for biosensing and includes the detection of DNA,[5,6] pathogens,[7] small molecules,[8] and metal ions.[9] Various Cas proteins of Class II, including Cas9,[10−13] Cas12,[14−17] Cas13,[18] and Cas14,[19] attracted much attention because of their simplicity that only a single effector is required.

Cas9 as one of the most extensively studied Cas effectors targets double-stranded DNA (dsDNA) by a single guided RNA (sgRNA).[20,21] Pardee *et al.* developed a NASBA-CRISPR method to visually differentiate ZIKV from dengue based on Cas9 cleavage-controlled translation of the LacZ enzyme, which can catalyze a color reaction of chlorophenol red-b-D-galactopyranoside.[22] Recently, gold nanoparticle (AuNP)-modified DNA probe-Cas9/sgRNA hybrids were used to label specific DNA targets and enabled visual DNA detection on paper.[23] Typically, Cas9 is a single-turnover enzyme that only recognizes dsDNA with a unique protospacer adjacent motif (PAM). Moreover, the selectivity of Cas9 highly depends on the position and number of the variable base (only the single-base variation in or close to PAM can be moderately differentiated), and non-target and non-canonical PAM could cause undesirable cleavage.[24] Both the inherent properties of Cas9 limited Cas9-mediated biosensing. Further, Cas12a that has single-stranded DNA (ssDNA) or ssDNA-activated *trans*-cleavage activity has also been confirmed to be used for visual DNA detection based on AuNP-labeled probes,[25] which indicate that the CRISPR/Cas system holds a great potential for point-of-care (POC) diagnosis.[26]

Cas13a is a high-fidelity, crRNA-guided, single-stranded RNA (ssRNA)-targeted RNase that can serve as an ideal candidate for RNA profiling.[27,28] Especially, specific recognition of target RNA can activate the *trans*-cleavage activity of Cas13a to non-specifically cleave nearby RNAs. Our previous work has confirmed that Cas13a has great selectivity for miRNA detection that even a single-base variation at the terminal of miRNA can be dramatically distinguished.[29] The most widely used qRT-PCR is sensitive and cost-effective while limited by the medium selectivity and the requirement of a well-designed reverse transcription primer to relatively hybridize with short miRNA stably. Relatively, high-fidelity Cas13a/crRNA can differentiate a single-base variation of miRNA through simply introducing a mismatch into the crRNA spacer,[29] without the assistance of a toxicant that affects DNA polymerase activity, as well as other complex and expensive modified probes. According to the transcendental characteristics of Cas13a, several fluorescence,[30,31] electrochemical,[32,33]

Received: September 1, 2020
Accepted: December 29, 2020
Published: January 7, 2021

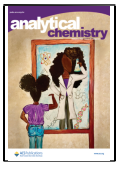

https://dx.doi.org/10.1021/acs.analchem.0c03708
Anal. Chem. 2021, 93, 2038−2044

Scheme 1. Principle Scheme of High-Fidelity CRISPR/Cas13a *trans*-Cleavage-Triggered Rolling Circle Amplified DNAzyme for Visual Profiling of microRNA

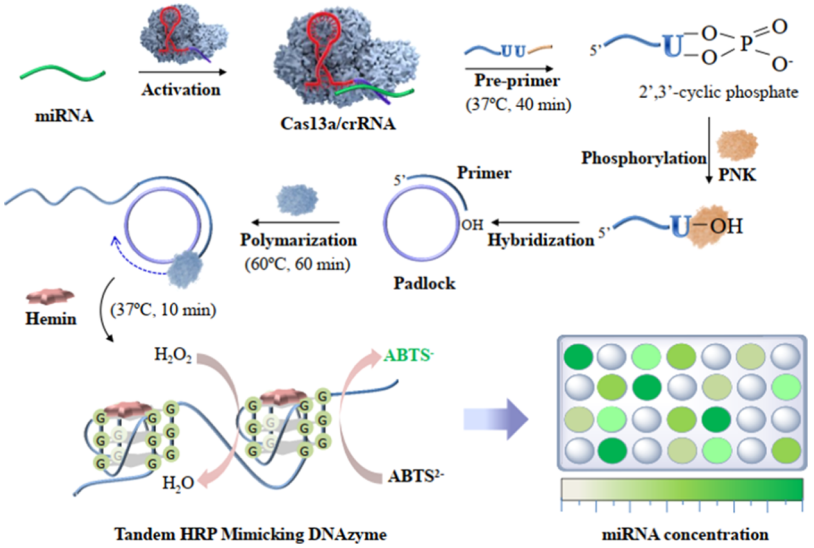

and electrochemiluminescence analysis platforms have been constructed.[34] Considering that these methods still require cumbersome instruments and expensive probes with modification (e.g., fluorophores, quenchers, methylene blue, and so forth), developing Cas13a-based visual miRNA detection could meet the demand of POC.

Herein, for the first time, we developed a Cas13a-based visual detection platform, termed as vCas, for sensitive and specific miRNA profiling. In principle (as shown in Scheme 1), Cas13a/crRNA collaterally cleaves the uracil ribonucleotide (rU)-bearing pre-primer upon recognition of target miRNA. Then, the remaining 5′-DNA fragment of the pre-primer can further initiate DNA polymerase-mediated rolling circle amplification (RCA) after its 3′-end is healed by T4 polynucleotide kinase (T4 PNK) and generate a long G-rich repeat sequence, which can form a tandem G-quadruplex that acts as horseradish peroxidase mimicking DNAzyme to catalyze the oxidation of the 2,2′-azino-bis (3-ethylbenzthiazoline-6-sulfonic acid) diammonium salt ($ABTS^{2-}$) in the presence of hemin and generate visible color change.[35,36] In this study, miR-10b, a potential biomarker that was confirmed to be highly expressed in metastatic breast cancer cells,[37,38] was chosen as a model target.[39−42] Benefiting from the excellent selectivity of Cas13a, the undesired non-target nucleic acid can be excluded from the amplification reaction. Moreover, this homogeneous method does not require a labeled probe, thereby reducing the complexity and cost of detection.

EXPERIMENTAL SECTION

Materials and Apparatus. T7 RNA polymerase, Bst DNA polymerase, T4 DNA ligase, exonuclease I, exonuclease III, and T4 polynucleotide kinase were provided by New England Biolabs (Beijing, CN). RNase free water, 10 mM dNTPmix, the RNase inhibitor, the 10× PCR buffer, and RNAiso for small RNA were purchased from Takara (Dalian, CN). Hemin, 2 mM each NTP mix, dimethyl sulfoxide, and an EL-ABTS Kit were purchased from Sangon (Shanghai, CN). DNA probes used in this study were synthesized by Sangon, and synthetic miRNAs were ordered from Takara. All the sequences are listed in Table S1. 96-well polystyrene microplates were purchased from Corning Costar Co., Ltd. (Germany). LbuCas13a was obtained according to our previous report.

Preparation of crRNA. crRNA was synthesized by T7 RNA polymerase-mediated *in vitro* transcription using a dsDNA template containing a T7 promoter. The transcription reaction was performed with 10 U/μL T7 RNA polymerase, 1 μM dsDNA template, 1 U/μL RNase inhibitor, and the 1× RNA polymerase reaction buffer at 37 °C for 6 h. The products was then purified using an RNA clean kit (Tiangen), followed by determining the concentration with a Nanodrop 2000 UV−vis spectrophotometer.

Preparation of a Circular Padlock Probe. For preparation of a circular padlock probe, 4 μM linear probe and a bridge DNA probe were added into 50 μL of the T4 DNA ligase buffer and incubated at 95 °C for 5 min and then slowly annealed to 25 °C with a speed of 2 °C/min. Then, 400 U T4 DNA ligase was added. The ligation reaction was carried out at 37 °C for 90 min. After that, 50 U exonuclease I and 125 U exonuclease III were added to digest unreacted linear DNA probes at 37 °C for 90 min in 1× NEBuffer I. Finally, the reaction was terminated by heating at 80 °C for 10 min. The obtained circular DNA padlock probe was purified using an oligo DNA purification kit (Sangon) and quantified using a Nanodrop 2000 and subsequently stored at −20 °C before use.

Cas13a-Based Cleavage Reaction and RCA. The 5 μL Cas13a cleavage reaction system contains target miRNA, 10 nM Cas13a protein, 5 nM crRNA, 100 nM pre-primer, and T4 PNK (0.5 U/μL) and was incubated in the 1× PCR buffer at 37 °C for 40 min. The obtained mature primer was then reacted with a 50 nM circular padlock probe, 0.5 U/μL Bst DNA polymerase in the 1× isothermal buffer (New England Biolabs) with a final volume of 10 μL at 60 °C for 1 h.

Colorimetric Detection. The abovementioned mixture was incubated with 10 μM hemin at 37 °C for 10 min. Subsequently, 40 μL of the ABTS solution was added and incubated at 37 °C for another 10 min. After adding 50 μL of the stop solution into the mixture, the detection results were estimated by the naked eye or the absorbance at 405 nm was measured using a microplate reader. In this article, all data were obtained from three repeated experiments.

https://dx.doi.org/10.1021/acs.analchem.0c03708
Anal. Chem. 2021, 93, 2038−2044

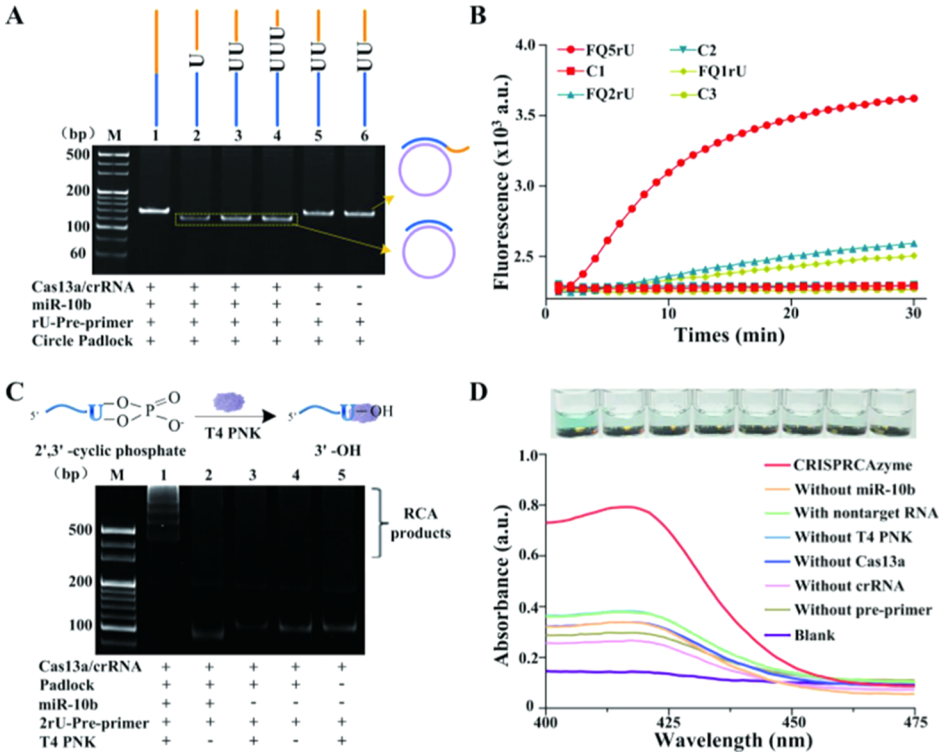

Figure 1. Feasibility analysis of vCas. (A) PAGE result of the *trans*-cleavage effect of Cas13a/crRNA on the pre-primer with different numbers of rU. (B) Real-time monitoring of the effect of Cas13a *trans*-cleavage on the three reporters with five, two, and one rU (FQ5rU, FQ2rU, and FQ1rU, respectively). C1, C2, and C3 are the corresponding control samples without miR-10b. The concentrations of Cas13a and miR-10b were 10 and 1 nM, respectively. All the three reporters were 100 nM. (C) PAGE analysis of the RCA products. M is the marker. (D) Image and absorption analysis results of vCas for miR-10b detection.

Extraction of Small RNA from Human Cell Lines and Human Peripheral-Blood Serum. All cell lines used in this paper were cultured in Dulbecco's modified Eagle's medium (Life) with 10% fetal bovine serum. The cells were collected through digestion and centrifugation when the cell density reached 70−80%. The total small RNA of the cells was obtained using a small RNA extraction kit (Takara) and quantified using the Nanodrop 2000 and stored at −80 °C for later use.

The peripheral-blood serum samples from one healthy human and breast cancer patient were derived from the First Affiliated Hospital of Guangzhou Medical University, Guangzhou, China. The total miRNA in serum was extracted using the Serum/Plasma miRNA extraction and isolation kit (Tiangen) and stored at −80 °C. This experiment conformed to the national and international medical experiment ethics standards.

RESULTS AND DISCUSSION

LbuCas13a used in this study prefers to cleave the rU neighboring phosphodiester bond. An oligo DNA bearing two rU (named "pre-primer") was designed to serve as the substrate of Cas13a/crRNA *trans*-cleavage. First, it is necessary to test whether target miRNA-activated Cas13a/crRNA can effectively cleave the pre-primer. A series of oligo DNAs with different numbers of rU were designed. The polyacrylamide gel electrophoresis (PAGE) result is shown in Figure 1A. Compared to the pre-primer without rU (lane 1), the three pre-primers with one (lane 2), two (lane 3), or three rU (lane 4) can be cleaved by miR-10b-activated Cas13a/crRNA, and their hybrids with the padlock have lower molecular weights. In addition, lane 2 shows a relatively weak band, which implies that the cleavage efficiency of Cas13a on the oligo with a single rU was obviously decreased. In addition, pre-primers with other ribonucleotides (rA, rC, and rG) have also been proven to be cleaved by miR-10b-activated Cas13a/crRNA, and the rU-bearing pre-primer was cleaved the most (Figure S1).

Next, the effect of the number of rU in the pre-primer on the *trans*-cleavage efficiency of Cas13a/crRNA was tested by real-time fluorescence monitoring. The results (Figure 1B) indicated that the fluorescence growth rate obviously decreases with the decrease of the rU number. Considering that too much rU may generate a primer with different lengths that affect subsequent polymerization reactions, the pre-primer with two rU was selected to execute vCas.

Moreover, the 5′-fragment of the pre-primer that was cleaved by miR-10b-activated Cas13a/crRNA was used to initiate the RCA reaction. However, the PAGE result showed that there was no amplification product. According to a previous report, Cas13 *trans*-cleavage generates two RNA fragments: one has a hydroxyl at its 5′-end and the other possesses a 2′,3′-cyclic phosphate at its 3′-end, which could hinder the action of DNA polymerase.[43] Thus, PNK was applied to transform the 5′-fragment of the pre-primer into a mature primer with a hydroxyl.[44] Figure 1C shows that compared to other samples without T4 PNK, the PNK-treated Cas13a-cleaved pre-primer can generate obvious RCA products, which indicated that T4 PNK-mediated removal of the 2′,3′-cyclic phosphate is the key to initiate DNA polymerization reaction.

Then, the RCA products were incubated with hemin and $ABTS^{2-}$. As a result, the colorless mix turned to green within

https://dx.doi.org/10.1021/acs.analchem.0c03708
Anal. Chem. 2021, 93, 2038−2044

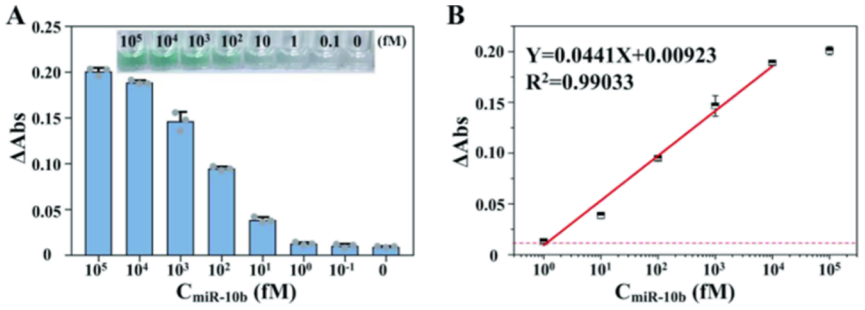

Figure 2. Sensitivity analysis of vCas. (A) ΔAbs of vCas with different concentrations of miR-10b (100 pM, 10 pM, 1 pM, 100 fM, 10 fM, 1 fM, 100 aM, and 0). (B) Linear analysis of vCas detection results for miR-10b. The red dashed line represents the LOD. The standard deviation was obtained from three batches of detection.

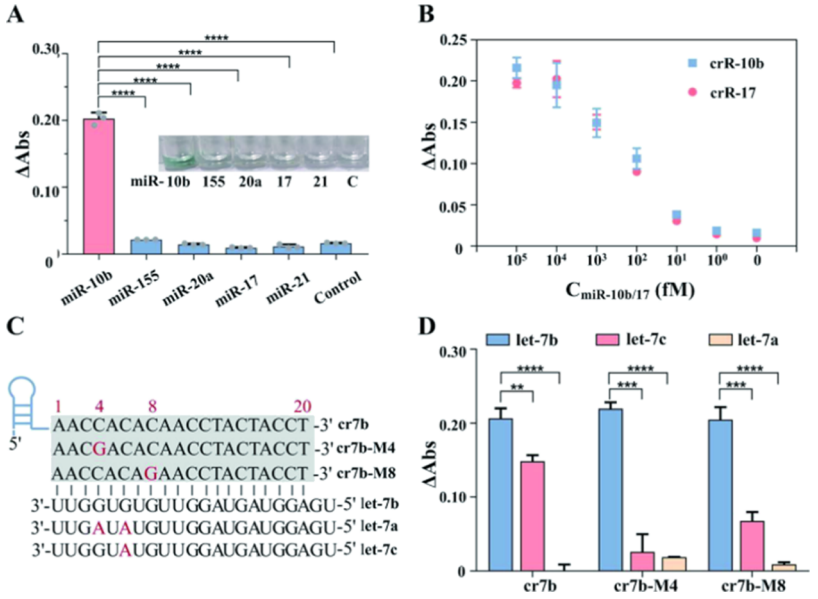

Figure 3. Specificity analysis of the performance of vCas. (A) Detection results of vCas for different miRNAs. (B) Absorption detection results for miR-10b and miR-17 when different concentrations (100 pM, 10 pM, 1 pM, 100 fM, 10 fM, and 0) of miR-10b and miR-17 coexist in a 1:1 ratio. (C) Sequences of a perfectly matched crRNA (cr7b), two crRNAs with a single mismatch at the site of 4 or 8 (cr7b-M4 and cr7b-M8), and three homologous let-7 family members (let-7b, let-7a, and let-7c). All the different bases in crRNA, let-7a, and let-7c are marked in red. (D) Absorbance analysis results of vCas with different crRNAs (crR7b, cr7b-M4, and cr7b-M8) for the three homologous let-7 family members (1 nM).

10 min. The photograph and the corresponding absorption spectroscopy results are shown in Figure 1D. It can be seen that only the complete vCas system with miR-10b (10 nM) displayed significant color change and enhancement of absorption intensity. Moreover, whether undesired ssDNA or dsDNA against the G-quadruplex could affect the detection results was tested (Figure S2). All the crRNA, padlock probe, and pre-primer that are critical components for vCas showed no significant contribution to the absorbance.

To evaluate the performance of vCas for miRNA detection, a series of diluted miR-10b were tested by vCas. The photograph and absorption spectroscopy results are shown in Figure 2A. The ΔAbs was obtained by subtracting the absorbance of the control sample without crRNA from the total absorbance value. As seen, the absorption intensity gradually increased with the increase of miR-10b concentration. Also, the ΔAbs values are linearly related to the logarithm of the miR-10b concentration from 1 fM to 10 pM (Figure 2B). The correlation equation is $\Delta Abs = 0.00923 + 0.0441 \times \lg C_{miR\text{-}10b}(fM)$ ($R^2 = 0.99033$). The limit of detection (LOD) (determined by 3 times of the standard deviation of the absorption detection results of the control sample without miR-10b) is 1 fM. Moreover, the sensitivity of vCas was compared to one-step Cas13a detection (Figure S3). The result confirmed that the vCas system can reach an LOD of 1 fM, which is 4 orders of magnitude lower than that of the one-step Cas13a detection method. Then, five different miRNAs, miR-10b, miR-155, miR-20a, miR-17, and miR-21, were introduced into the vCas system to evaluate the specificity. The colorimetric and absorption detection results (Figure 3A) showed that only miR-10b can cause obvious color change and dramatic enhancement of absorbance. Also, we respectively detect miR-10b and miR-17 by vCas when miR-10b and miR-17 coexisted in the system with a ratio of 1:1. Figure 3B shows that the detection results for miR-10b and miR-17 were consistent.

Further, we attempted to distinguish let-7b from its two highly homologous family members (let-7a and let-7c, sequences shown in Figure 3C) by vCas. To improve the specificity of Cas13a/crRNA, an extra mismatch was introduced into the 4 or 8 site of the spacer of crRNA (cr7b-M4 and cr7b-M8) to decrease the tolerance of Cas13a/

https://dx.doi.org/10.1021/acs.analchem.0c03708
Anal. Chem. 2021, 93, 2038−2044

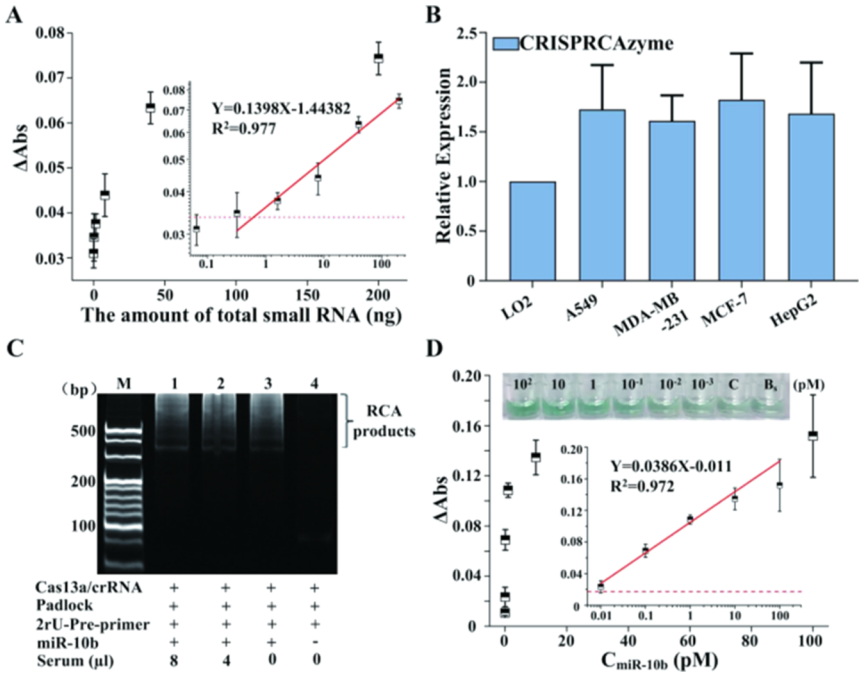

Figure 4. Performance of vCas for detecting miRNA in complex samples. (A) Sensitivity analysis of vCas by detecting miR-10b in different amounts of total small RNA extracted from MCF-7 cells. (B) Comparison of the expression level of miR-10b in different cancer cell lines by vCas. LO2 was used as the control, and the miR-10b expression level of LO2 was set to 1. (C) PAGE analysis of Cas13a-mediated RCA reaction in different volumes of total RNA extracted from human peripheral-blood serum (8 and 4 μL) with 100 pM synthetic miR-10b. (D) Sensitivity analysis of vCas by detecting different concentrations of miR-10b (1 fM ~ 100 pM) in 10× diluted serum samples. C is the control sample without added miR-10b. B_s is the vCas sample without crRNA.

crRNA for mismatch. The absorption detection results are shown in Figure 3D. As seen, Cas13a/cr7b can efficiently distinguish let-7b from let-7a that has two base differences to let-7b, while let-7c that has only a single base difference to let-7b also contribute to obvious enhancement of absorbance. Relatively, both Cas13a/cr7b-M4 and Cas13a/cr7b-M8 can significantly distinguish let-7b from let-7a and let-7c. These results indicate that vCas can provide single-base specificity by flexibly introducing an extra mismatch into the targeting region of the crRNA.

In addition, to investigate the validity of vCas for detecting miRNA in the real sample, different amounts of total small RNA extracted from the human breast adenocarcinoma cell line (MCF-7) were analyzed by vCas. As shown in Figure 4A, miR-10b in 1.6 ng of total small RNA can be detected. Further, miR-10b extracted from four human cell lines, including the human lung carcinoma cell line (A549), human breast adenocarcinoma cell lines (MDA-MB-231 and MCF-7), and the human hepatocellular liver carcinoma cell line (HepG2), were analyzed by vCas. The human normal cell line (LO2) was used as the control. The detection results in Figure 4B showed that all the four cancer cells displayed varying degrees of overexpression of miR-10b compared to LO2.

Next, we tested the application ability of vCas for detecting miR-10b in human peripheral-blood serum. PAGE results (Figure 4C) showed that the total RNA sample extracted from human peripheral-blood serum with 100 pM synthetic miR-10b can generate significant RCA products. 8 μL of serum total RNA extracts has no obvious effect on the amount of RCA products. Then, a series of miR-10b with different concentrations were spiked into 10× diluted serum and detected by vCas. The results of absorption detection in Figure 4D showed that vCas maintained a good linearity from 10 fM to 100 pM and achieved a detection limit of 10 fM, which is 10-fold lower than detecting miR-10b in the buffer. Compared to the sample without crRNA (sample B_s), the 10× diluted serum sample without added miR-10b (sample C) showed a darker color, which indicated that other substances in the serum can cause the increase of background signal.

CONCLUSIONS

In summary, we developed a CRISPR/Cas13a-based visual miRNA detection method, termed as vCas, in which a pre-primer was designed to be as the *trans*-cleavage substrate of Cas13a/crRNA and serve as a primer for RCA after being healed by T4 PNK. Through this method, target miRNA can be quantified by the naked eye. The detection results confirmed that vCas can provide a detection limit of 1 fM for miR-10b with a good linearity from 1 fM to 10 pM. Also, highly homologous let-7 family members that only have a single base difference can be significantly distinguished. Especially, miR-10b in cell extracts and serum can be reliably detected. Previous studies indicate that the Cas13a-based biosensing method possesses a broad application prospect, including detecting long viral RNA[45] and even intact bacteria cells.[7] Although the number of the available Cas protein types and the cross-reaction among different Cas13a proteins limited the application of Cas13a in multiplex detection, multichannel microfluidic chips could solve the problem. However, multi-step processing steps bring inconvenience to the automation development of vCas. Further simplifying the reaction process will facilitate the application of vCas in automated high-throughput detection.

https://dx.doi.org/10.1021/acs.analchem.0c03708
Anal. Chem. 2021, 93, 2038−2044

■ ASSOCIATED CONTENT

Supporting Information

The Supporting Information is available free of charge at https://pubs.acs.org/doi/10.1021/acs.analchem.0c03708.

List of the sequences for vCas, analysis of Cas13a/crRNA *trans*-cleavage efficiency to four pre-primers, analysis of the effect of undesired DNA on detection results, and linear analysis of the one-step Cas13a method for miR-10b detection (PDF)

■ AUTHOR INFORMATION

Corresponding Authors

Ru Huang − *MOE Key Laboratory of Laser Life Science & Institute of Laser Life Science, College of Biophotonics, South China Normal University, Guangzhou 510631, PR China; Guangdong Provincial Key Laboratory of Laser Life Science, College of Biophotonics, South China Normal University, Guangzhou 510631, PR China*; Phone: (+86) 20 8521 1436; Email: huangru@scnu.edu.cn

Da Xing − *MOE Key Laboratory of Laser Life Science & Institute of Laser Life Science, College of Biophotonics, South China Normal University, Guangzhou 510631, PR China; Guangdong Provincial Key Laboratory of Laser Life Science, College of Biophotonics, South China Normal University, Guangzhou 510631, PR China*; orcid.org/0000-0001-9752-8458; Email: xingda@scnu.edu.cn

Authors

Ting Zhou − *MOE Key Laboratory of Laser Life Science & Institute of Laser Life Science, College of Biophotonics, South China Normal University, Guangzhou 510631, PR China; Guangdong Provincial Key Laboratory of Laser Life Science, College of Biophotonics, South China Normal University, Guangzhou 510631, PR China*

Mengqi Huang − *MOE Key Laboratory of Laser Life Science & Institute of Laser Life Science, College of Biophotonics, South China Normal University, Guangzhou 510631, PR China; Guangdong Provincial Key Laboratory of Laser Life Science, College of Biophotonics, South China Normal University, Guangzhou 510631, PR China*

Jinqiong Lin − *Department of Laboratory Medicine, The First Affiliated Hospital of Guangzhou Medical University, Guangzhou 510631, PR China*

Complete contact information is available at: https://pubs.acs.org/10.1021/acs.analchem.0c03708

Author Contributions

T.Z. and M.H. contributed equally to this work. All authors have given approval to the final version of the manuscript.

Notes

The authors declare no competing financial interest.

■ ACKNOWLEDGMENTS

We give special thanks to Prof. Yanli Wang from the Institute of Biophysics, Chinese Academy of Sciences, for supply of the pET-Sumo-LbuCas13a expression plasmid. This work was supported by the National Natural Science Foundation of China (NSFC) (81630046), the Natural Science Foundation of Guangdong Province, China (2020A1515010525), and the Science and Technology Program of Guangzhou (2019050001).

■ REFERENCES

(1) Kirchner, M.; Schneider, S. *Angew. Chem., Int. Ed.* **2015**, *54*, 13508−13514.
(2) Adli, M. *Nat. Commun.* **2018**, *9*, 1911.
(3) Tang, W.; Hu, J. H.; Liu, D. R. *Nat. Commun.* **2017**, *8*, 15939.
(4) Wang, Q.; Liu, X.; Zhou, J.; Yang, C.; Wang, G.; Tan, Y.; Wu, Y.; Zhang, S.; Yi, K.; Kang, C. *Adv. Sci.* **2019**, *6*, 1901299.
(5) Li, Y.; Li, S.; Wang, J.; Liu, G. *Trends Biotechnol.* **2019**, *37*, 730−743.
(6) Kaminski, M. M.; Alcantar, M. A.; Lape, I. T.; Greensmith, R.; Huske, A. C.; Valeri, J. A.; Marty, F. M.; Klämbt, V.; Azzi, J.; Akalin, E.; Riella, L. V.; Collins, J. J. *Nat. Biomed. Eng.* **2020**, *4*, 601−609.
(7) Shen, J.; Zhou, X.; Shan, Y.; Yue, H.; Huang, R.; Hu, J.; Xing, D. *Nat. Commun.* **2020**, *11*, 267.
(8) Iwasaki, R. S.; Batey, R. T. *Nucleic Acids Res.* **2020**, *48*, No. e101.
(9) Xiong, Y.; Zhang, J.; Yang, Z.; Mou, Q.; Ma, Y.; Xiong, Y.; Lu, Y. *J. Am. Chem. Soc.* **2020**, *142*, 207−213.
(10) Wang, T.; Liu, Y.; Sun, H. H.; Yin, B. C.; Ye, B. C. *Angew. Chem., Int. Ed.* **2019**, *58*, 5382−5386.
(11) Zhou, W.; Hu, L.; Ying, L.; Zhao, Z.; Chu, P. K.; Yu, X.-F. *Nat. Commun.* **2018**, *9*, 5012.
(12) Zhang, K.; Deng, R.; Li, Y.; Zhang, L.; Li, J. *Chem. Sci.* **2016**, *7*, 4951−4957.
(13) Wang, R.; Zhao, X.; Chen, X.; Qiu, X.; Qing, G.; Zhang, H.; Zhang, L.; Hu, X.; He, Z.; Zhong, D.; Wang, Y.; Luo, Y. *Anal. Chem.* **2020**, *92*, 2176−2185.
(14) Dai, Y.; Somoza, R. A.; Wang, L.; Welter, J. F.; Li, Y.; Caplan, A. I.; Liu, C. C. *Angew. Chem., Int. Ed.* **2019**, *58*, 17399−17405.
(15) Chen, J. S.; Ma, E.; Harrington, L. B.; Da Costa, M.; Tian, X.; Palefsky, J. M.; Doudna, J. A. *Science* **2018**, *360*, 436.
(16) Peng, S.; Tan, Z.; Chen, S.; Lei, C.; Nie, Z. *Chem. Sci.* **2020**, *11*, 7362−7368.
(17) Yin, K.; Ding, X.; Li, Z.; Zhao, H.; Cooper, K.; Liu, C. *Anal. Chem.* **2020**, *92*, 8561−8568.
(18) Chen, Q.; Tian, T.; Xiong, E.; Wang, P.; Zhou, X. *Anal. Chem.* **2020**, *92*, 573−577.
(19) Harrington, L. B.; Burstein, D.; Chen, J. S.; Paez-Espino, D.; Ma, E.; Witte, I. P.; Cofsky, J. C.; Kyrpides, N. C.; Banfield, J. F.; Doudna, J. A. *Science* **2018**, *362*, 839.
(20) Jinek, M.; Chylinski, K.; Fonfara, I.; Hauer, M.; Doudna, J. A.; Charpentier, E. *Science* **2012**, *337*, 816.
(21) Li, Y.; Teng, X.; Zhang, K.; Deng, R.; Li, J. *Anal. Chem.* **2019**, *91*, 3989−3996.
(22) Pardee, K.; Green, A. A.; Takahashi, M. K.; Braff, D.; Lambert, G.; Lee, J. W.; Ferrante, T.; Ma, D.; Donghia, N.; Fan, M.; Daringer, N. M.; Bosch, I.; Dudley, D. M.; O'Connor, D. H.; Gehrke, L.; Collins, J. J. *Cell* **2016**, *165*, 1255−1266.
(23) Wang, X.; Xiong, E.; Tian, T.; Cheng, M.; Lin, W.; Wang, H.; Zhang, G.; Sun, J.; Zhou, X. *ACS Nano* **2020**, *14*, 2497−2508.
(24) Hsu, P. D.; Scott, D. A.; Weinstein, J. A.; Ran, F. A.; Konermann, S.; Agarwala, V.; Li, Y.; Fine, E. J.; Wu, X.; Shalem, O.; Cradick, T. J.; Marraffini, L. A.; Bao, G.; Zhang, F. *Nat. Biotechnol.* **2013**, *31*, 827−832.
(25) Yuan, C.; Tian, T.; Sun, J.; Hu, M.; Wang, X.; Xiong, E.; Cheng, M.; Bao, Y.; Lin, W.; Jiang, J.; Yang, C.; Chen, Q.; Zhang, H.; Wang, H.; Wang, X.; Deng, X.; Liao, X.; Liu, Y.; Wang, Z.; Zhang, G.; et al. *Anal. Chem.* **2020**, *92*, 4029−4037.
(26) Halawa, M. I.; Li, B. S.; Xu, G. *ACS Appl. Mater. Interfaces* **2020**, *12*, 32888−32897.
(27) Abudayyeh, O. O.; Gootenberg, J. S.; Konermann, S.; Joung, J.; Slaymaker, I. M.; Cox, D. B. T.; Shmakov, S.; Makarova, K. S.; Semenova, E.; Minakhin, L.; Severinov, K.; Regev, A.; Lander, E. S.; Koonin, E. V.; Zhang, F. *Science* **2016**, *353*, aaf5573.
(28) East-Seletsky, A.; O'Connell, M. R.; Knight, S. C.; Burstein, D.; Cate, J. H. D.; Tjian, R.; Doudna, J. A. *Nature* **2016**, *538*, 270−273.
(29) Shan, Y.; Zhou, X.; Huang, R.; Xing, D. *Anal. Chem.* **2019**, *91*, 5278−5285.
(30) Gootenberg, J. S.; Abudayyeh, O. O.; Lee, J. W.; Essletzbichler, P.; Dy, A. J.; Joung, J.; Verdine, V.; Donghia, N.; Daringer, N. M.;

Freije, C. A.; Myhrvold, C.; Bhattacharyya, R. P.; Livny, J.; Regev, A.; Koonin, E. V.; Hung, D. T.; Sabeti, P. C.; Collins, J. J.; Zhang, F. *Science* **2017**, *356*, 438.
(31) Chen, M.; Luo, R.; Li, S.; Li, H.; Qin, Y.; Zhou, D.; Liu, H.; Gong, X.; Chang, J. *Anal. Chem.* **2020**, *92*, 13336−13342.
(32) Bruch, R.; Baaske, J.; Chatelle, C.; Meirich, M.; Madlener, S.; Weber, W.; Dincer, C.; Urban, G. A. *Adv. Mater.* **2019**, *31*, 1905311.
(33) Ma, X.; Li, M.; Tong, P.; Zhao, C.; Li, J.; Xu, G. *Biosens. Bioelectron.* **2020**, *156*, 112150.
(34) Zhou, T.; Huang, R.; Huang, M.; Shen, J.; Shan, Y.; Xing, D. *Adv. Sci.* **2020**, *7*, 1903661.
(35) Albada, H. B.; Golub, E.; Willner, I. *Chem. Sci.* **2016**, *7*, 3092−3101.
(36) Ma, D.-L.; Wang, M.; He, B.; Yang, C.; Wang, W.; Leung, C.-H. *ACS Appl. Mater. Interfaces* **2015**, *7*, 19060−19067.
(37) Singh, R.; Pochampally, R.; Watabe, K.; Lu, Z.; Mo, Y.-Y. *Mol. Cancer* **2014**, *13*, 256.
(38) Ma, L. *Breast Cancer Res.* **2010**, *12*, 210.
(39) Yoo, B.; Kavishwar, A.; Ross, A.; Wang, P.; Tabassum, D. P.; Polyak, K.; Barteneva, N.; Petkova, V.; Pantazopoulos, P.; Tena, A.; Moore, A.; Medarova, Z. *Cancer Res.* **2015**, *75*, 4407.
(40) Wang, F.; Fu, C.; Huang, C.; Li, N.; Wang, Y.; Ge, S.; Yu, J. *Biosens. Bioelectron.* **2020**, *150*, 111917.
(41) Zheng, X.; Li, L.; Zhang, L.; Xie, L.; Song, X.; Yu, J. *Biosens. Bioelectron.* **2020**, *147*, 111769.
(42) Li, Z.; Yang, H.; Hu, M.; Zhang, L.; Ge, S.; Cui, K.; Yu, J.; Yu, J. *ACS Appl. Mater. Interfaces* **2020**, *12*, 17177−17184.
(43) Gootenberg, J. S.; Abudayyeh, O. O.; Kellner, M. J.; Joung, J.; Collins, J. J.; Zhang, F. *Science* **2018**, *360*, 439.
(44) Das, U.; Shuman, S. *Nucleic Acids Res.* **2012**, *41*, 355−365.
(45) Ackerman, C. M.; Myhrvold, C.; Thakku, S. G.; Freije, C. A.; Metsky, H. C.; Yang, D. K.; Ye, S. H.; Boehm, C. K.; Kosoko-Thoroddsen, T.-S. F.; Kehe, J.; Nguyen, T. G.; Carter, A.; Kulesa, A.; Barnes, J. R.; Dugan, V. G.; Hung, D. T.; Blainey, P. C.; Sabeti, P. C. *Nature* **2020**, *582*, 277−282.

https://dx.doi.org/10.1021/acs.analchem.0c03708
Anal. Chem. 2021, 93, 2038−2044